PMU Measurements for Oscillation Monitoring: Connecting Prony Analysis with Observability

Anas Almunif, *Student Member, IEEE*, Lingling Fan, *Senior Member, IEEE*

***Abstract*—The objective of this paper is to rank phasor measurement unit (PMU) measurements for oscillation monitoring based on two approaches: oscillation mode observability and Prony analysis. In the first approach, the system model is assumed known and the critical oscillation mode observability of different measurements are compared. In the second approach, the dynamic model of the system is not known. Prony analysis is employed to identify critical oscillation modes based on PMU measurements. Measurements at different locations are compared for their characteristics in Prony analysis. Specifically, singular values of Hankel matrices are compared. The two approaches lead to the same conclusion. Their internal connection is presented in this paper. As a step further, sensitivity analysis of model order assumption and noise level in Prony analysis is conducted to show singular values of Hankel matrices can indeed serve as indicators of the quality of oscillation monitoring.**

***Index Terms*—PMU measurements, Prony analysis, observability, Hankel matrix, singular values.**

I. Introduction

PHASOR measurement units (PMUs) have been put into power grid for real-time monitoring. Using PMU data to identify electromechanical oscillations has been studied in the literature and an IEEE PES taskforce report [1] has been published in 2012. For ringdown signals, or measurements captured for a transient event, Prony analysis and Eigensystem Realization Algorithm (ERA) are two measurement-based identification methods [2]. More specifically, Prony analysis has been introduced in power system oscillation mode estimation in 1980s by J. Hauer [3]. As an extension, Prony analysis based on multiple channel data was presented in [4]. In the authors' prior work [5], multiple channel Prony analysis was formulated as a weighted least squares estimation problem with the weights obtained from single-channel Prony analysis. The estimation accuracy shows significant improvement.

Prony analysis accuracy also depends on the specification of system model order and sampling rate. Experiments have been conducted on Prony analysis to show the influence of model order and sampling rate on oscillation estimation accuracy [6]. The remarks on sampling rate influence on experiments in [6] are corroborated based on the analysis carried out in [7].

The objective of this paper is to examine estimation accuracy of Prony analysis and relate the indicator of accuracy to the physical system dynamic analysis.

Prony analysis is essentially to solve a least squares estimation (LSE) problem notated as $Da = Y$ where D is the Hankel matrix built upon measurements, Y is the measurement vector, and a is the parameter vector to be found. Since the solution of the overdetermined problem $\hat{a}$ is determined by the normal equation: $\hat{a} = (D^T D)^{-1} D^T Y$, a larger conditional number of $D^T D$ (the ratio of the maximal singular value versus the minimum) indicates a worse estimation accuracy. In ERA, singular value decomposition (SVD) of Hankel matrices will be conducted to construct dynamic system matrices. The above information indicates that singular values of Hankel matrices can give indication regarding estimation accuracy. A paper in 2013, indeed relies on SVD of Hankel matrices to judge PMU placement for dynamic stability assessment [8].

To investigate how singular values of a Hankel matrix relate to a physical system model, we use dynamic modeled-based observability to rank measurements generated from a known system model. The rank based on the observability will be shown to match the rank based on Hankel matrix singular values.

To this end, it is clear that the singular values of a Hankel matrix reflect signal observability of oscillation modes and hence they provide reasonable indication of estimation accuracy. Built upon this knowledge, we further studied the sensitivity of system model order assumption and noise level on estimation accuracy using the singular value plots.

The rest of the paper is organized as follows. Section II gives a brief introduction on Prony analysis. Section III presents modal decomposition based observability computation. Section IV presents test case results using the two approaches: observability computing based on a known dynamic model and measurement-based Hankel matrix singular value computation. Section V concludes the paper.

II. Prony analysis

A. Prony Analysis

Consider a Linear-Time Invariant (LTI) system with the initial state of $x(0) = x_0$ at time $t = 0$ second. If the input is removed from the system, the dynamic model can be expressed as the follows.

$$\dot{x}(t) = Ax(t) \tag{1}$$

$$y(t) = Cx(t) \tag{2}$$

where $y \in \mathbb{R}$ is defined as the output of the system, $x \in \mathbb{R}^n$ is the state of the system, $A \in \mathbb{R}^{n \times n}$ and $C \in \mathbb{R}^{1 \times n}$ are system matrices. The order of the system is defined by n. If the λ_i, p_i, and q_i are the i-th eigenvalue, the corresponding right eigenvector, and left eigenvectors of A respectively, (1)

A. Almunif and L. Fan are with the Department of Electrical Engineering, University of South Florida, Tampa, FL 33420 USA e-mail: linglingfan@usf.edu.

can be represented as:

$$x(t) = \sum_{i=1}^{n} (q_i^T x_0) p_i e^{\lambda_i t} = \sum_{i=1}^{n} R_i x_0 e^{\lambda_i t} \tag{3}$$

where $R_i = p_i q_i^T$ is a residue matrix. Based on (2), the $y(t)$ can be expressed as:

$$y(t) = \sum_{i=1}^{n} C R_i x_0 e^{\lambda_i t}. \tag{4}$$

The observed or measured $y(t)$ consists of $N+1$ samples which are equally spaced by Δt as: $y(t_k) = y(k), k = 0, ..., N$. (4) can be written in the exponential form as:

$$\hat{y}(t_k) = \sum_{i=1}^{n} C R_i e^{\lambda_i k \Delta t} = \sum_{i=1}^{n} C R_i z_i^k, \quad k = 1, ..., N \tag{5}$$

where z_i is the eigenvalues of the system in discrete time domain and $z_i = e^{\lambda_i \Delta t}$.

Note that z_i $(i = 1, \cdots, n)$ are the roots of the n-th characteristic polynomial function of the system as follows.

$$z^n - (a_1 z^{n-1} + a_2 z^{n-2} + ... + a_n z^0) = 0. \tag{6}$$

While the roots z_i might be complex numbers, the system polynomial coefficients a_i are real numbers.

From (6), we have

$$z^n = a_1 z^{n-1} + a_2 z^{n-2} + ... + a_n z^0. \tag{7}$$

A linear prediction model (8) can be formulated since $y(k)$ is the linear combination of z_i^k based on (5). Therefore,

$$y(n) = a_1 y(n-1) + a_2 y(n-2) + ... + a_n y(0). \tag{8}$$

Enumerating the signal samples from step n to step N, we have (9): $Y = Da$.

$$\underbrace{\begin{bmatrix} y(n) \\ \vdots \\ y(n+k) \\ \vdots \\ y(N) \end{bmatrix}}_{Y} = \underbrace{\begin{bmatrix} y(n-1) & \cdots & y(0) \\ \vdots & \ddots & \vdots \\ y(n+k-1) & \cdots & y(k) \\ \vdots & \ddots & \vdots \\ y(N-1) & \cdots & y(N-n) \end{bmatrix}}_{D} \underbrace{\begin{bmatrix} a_1 \\ \vdots \\ a_k \\ \vdots \\ a_n \end{bmatrix}}_{a} \tag{9}$$

The best estimate of a is found from the following normal equation.

$$\hat{a} = (D^T D)^{-1} D^T Y. \tag{10}$$

B. Singular Value Decomposition of the D Matrix

The SVD of the D matrix of the Prony analysis is the factorization of this matrix into the product of three matrices, and can be expressed as follows.

$$D = U \Sigma V^* \tag{11}$$

The dimension of D is $(N-n+1) \times n$. where U is $(N-n+1) \times (N-n+1)$ matrix, Σ is $(N-n+1) \times n$ diagonal matrix of positive real singular values of matrix D, and V^* is the conjugate transpose of V which is $n \times n$ matrix. U and V are unitary matrices, and the diagonal matrix Σ is given by the follows.

$$\Sigma = \begin{bmatrix} \Sigma_1 \\ 0 \end{bmatrix}, \ n \leq (N-n+1) \tag{12}$$

where Σ_1 is the diagonal of $\{\sigma_1, \sigma_2, \cdots, \sigma_n\}$, and note that $\sigma_1 \geq \sigma_2 \geq \cdots \geq \sigma_n$.

III. Observability of Modes

A. Modal decomposition

The system matrix A has the following characteristic related to an eigenvalue λ_i:

$$A v_i = \lambda_i v_i \tag{13}$$

where v_i is right eigenvector associated with λ_i. Then (13) can be represented as the following:

$$A \underbrace{\begin{bmatrix} v_1, v_2, \ldots, v_n \end{bmatrix}}_{V} = \begin{bmatrix} \lambda_1 v_1 & \lambda_2 v_2 & \ldots & \lambda_n v_n \end{bmatrix} = V \Lambda \tag{14}$$

where V is the right eigenvector matrix and $\Lambda = \text{diag}\{\lambda_1, \cdots, \lambda_n\}$. We may further find

$$\Lambda = V^{-1} A V \tag{15}$$

$$A = V \Lambda V^{-1}. \tag{16}$$

The dynamic model can be expressed by the following:

$$\dot{x}(t) = V \Lambda V^{-1} x(t) \tag{17}$$

Define $\tilde{x} = V^{-1} x$ (or $x = V\tilde{x}$), then the dynamic system represented by $\tilde{X}$ is as follows.

$$\begin{aligned} &\dot{\tilde{x}}(t) = \Lambda \tilde{x}(t), \ \text{Or:} \\ &\dot{\tilde{x}}_i(t) = \lambda_i \tilde{x}_i(t) \end{aligned} \tag{18}$$

The time domain expression of every element of the new state vector $\tilde{x}$ can be found independently with the i-th eigenvalue:

$$\tilde{x}_i(t) = e^{\lambda_i t} \tilde{x}_i(0) \tag{19}$$

The output of the system will be expressed as the following:

$$y(t) = CV\tilde{x}(t) = CV \begin{bmatrix} \tilde{x}_1(0) e^{\lambda_1 t} \\ \vdots \\ \tilde{x}_n(t) e^{\lambda_n t} \end{bmatrix} = \sum_{i=1}^{n} \Omega_i \tilde{x}_i(0) e^{\lambda_i t} \tag{20}$$

where $\Omega = CV$ is the observability row vector corresponding to each eigenvalue.

From the output or measurement expression $y(t)$, it can be seen that for the same initial condition notated by $x(0)$ and further $\tilde{x}(0)$, different measurements will have different observability of each eigenvalue. Thus, Ω will be computed for measurements and $|\Omega_i|$ will be used to rank the measurements based on their observability to the i-th eigenvalue.

IV. Case Studies

The two approaches for measurement ranking will be applied to two systems: the 2-area 4-machine case and the 16-machine 68-bus system. The measurement data are generated using the power system toolbox (PST) [9]. PST also has the capability to conduct small-signal perturbation and give the linear system matrices. The observability vectors are computed based on the system matrices obtained. Though MATLAB's signal processing toolbox has a Prony analysis function that can give a discrete system transfer function from a given time-series signal, it does not provide the intermediate information regarding Hankel matrix. As such, an in-house Prony analysis toolbox developed for [5], [10] is utilized to conduct Prony analysis, including least squares estimation to find coefficient vector a, eigenvalue computing, and signal reconstruction.

A. Two-area four-machine system

The classic two-area four machine system for inter-area oscillation study (shown in Fig. 1) is used for the first case study. The four generators are assumed to have a second-order swing dynamics each. Twenty seconds simulation is conducted for a short-circuit transient event. The measurements are resampled to have equal time steps.

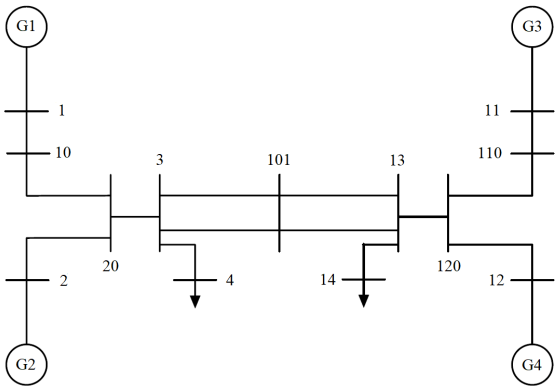

Fig. 1: The two-area four machine test case in PST.

TABLE I
The observability approach of buses 1, 13, and 101 with damping ratio and frequency of the 13-bus system.

Mode	Observability			Damping Ratio	Frequency (Hz)
	Bus 1	Bus 13	Bus 101		
1	0.04	0.02	0.11	0.00	0.56
2	0.05	0.04	0.04	-0.00	1.20
3	0.03	0.05	0.06	0.00	1.21

a) Comparison of different signals: The sampling rate is chosen to be 0.03 s. Three voltage signals for three different buses (buses 1, 13, and 101) are selected. Research in [11] has a given detailed analysis on interarea oscillation observability for buses on a radial path. It is found that the bus located in the middle of the path is shown to have the best observability. In turn, Bus 101 is expected to have the largest absolute value for its observability corresponding to the inter-area oscillation mode.

This is confirmed by the observability analysis conducted base on the linear system matrices. The observability along with the damping ratio, and frequency of the system modes are also presented in Table I. In this system, three oscillation modes are identified and shown in Table I: 0.56 Hz inter-area oscillation mode and two local oscillation modes at 1.20 Hz and 1.21 Hz. We can see clearly that Bus 101 has a larger observability on the 0.56 Hz mode than the other two buses.

It is known that the angle difference between the buses located in two areas should better reflect inter-area oscillations compared to the angle difference between two buses located in the same area. In addition to the three voltage signals, three angle difference signals are also selected: $\theta_2-\theta_1$, $\theta_{11}-\theta_1$, and $\theta_{11}-\theta_{12}$. Since PST does not give the measurement matrix on the bus angles, the observability for angle differences is omitted.

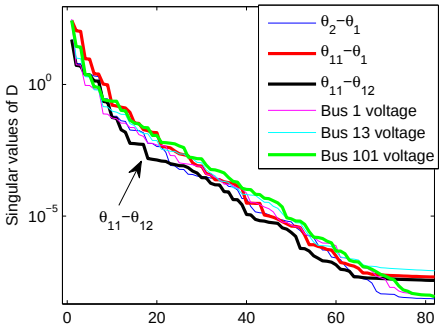

Fig. 2: Singular values for the Hankel matrices related to the six signals. The system order is 220.

The Hankel matrices D of the six selected signals are built based on the simulation data. Fig. 2 shows the singular values of the D matrices of the three voltage signals and the three angle signals. It can be clearly seen that the singular values related to Bus 101 (in the middle of the path) and the angle difference of buses in two areas ($\theta_{11} - \theta_1$) have singular values on the top. On the other hand, angle difference for two buses located in one area ($\theta_{11} - \theta_{12}$) is on the bottom of the chart. The singular value plots confirm that Bus 101's voltage magnitude and the angle between two areas have the best observability of interarea oscillation mode.

Fig. 3 presents the reconstructed signals against the original measurements (thin blue lines).

b) Comparison of model order assumption: For the angle difference signal ($\theta_{11} - \theta_{12}$) related to two buses in Area 2, Prony analysis with different model order assumptions are carried out. The model order is assumed to be 50, 120 and 220, respectively. The singular value plots of the corresponding Hankel matrices are shown in Fig. 4.

The singular value plots clearly show that high-order results in better estimation accuracy. This point has been recognized generally (see [12] Chapter 10). The reconstructed signals are presented in Fig. 5. It can be seen that high order assumption results in better match between the reconstructed signal and the original signal.

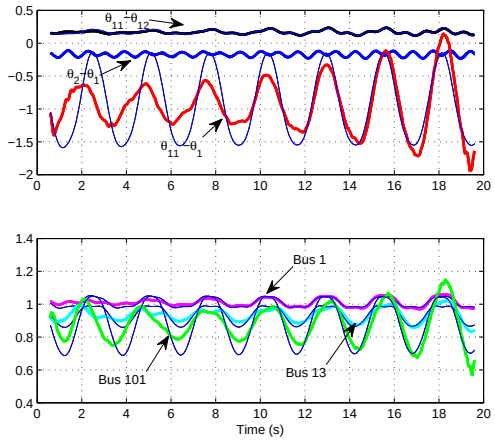

Fig. 3: Comparison of the reconstructed signals against the original measurements (thin blue lines).

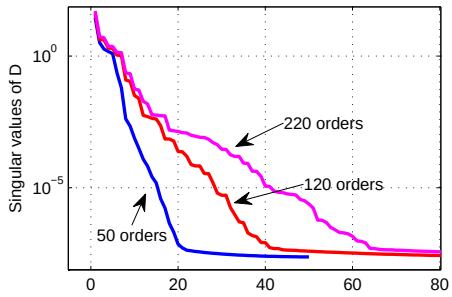

Fig. 4: Singular values for the Hankel matrices related to three orders: 50, 120 and 220.

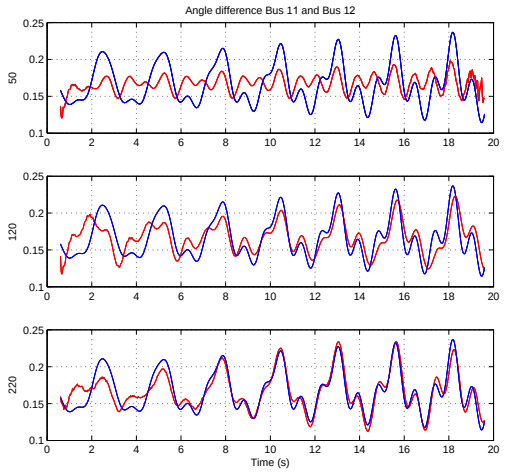

Fig. 5: Comparison of the reconstructed signals against the original measurements for different model order assumptions. Blue lines are the original measurements while the red lines are the reconstructed signals.

B. 16-Machine 68-Bus System

A larger power system, which is the 16-machine, 68-bus system, is used to further validate that both of the observability calculation and Prony analysis singular value examination lead to the same findings. This system is a reduced model of the New England Test System (NETS)-New York Power System

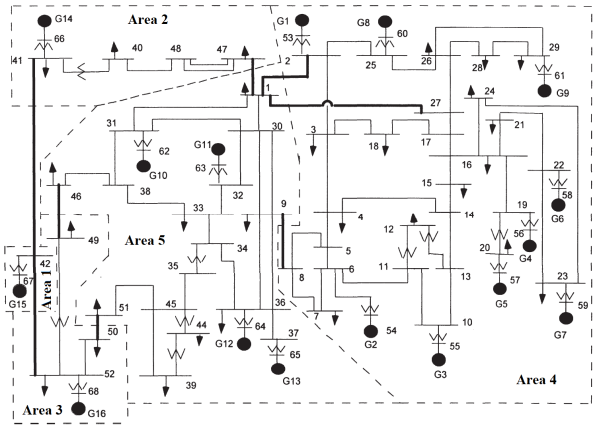

Fig. 6: 16-machine, 68-bus test case [13].

(NYPS) interconnected system [13] and has five areas. NETS is represented by area 4 which has generators G1 to G9, while NYPS is represented by area 5 which has generators G10 to G13 as shown in Fig. 6. The other three areas have equivalent generators G14 to G16.

Three voltage signals in different areas are chosen: Bus 5, Bus 29, and Bus 67. Their observability related to four modes with lowest frequencies are computed and the results are shown in Fig. 7. From this figure, it can be seen that Bus 29 is more observable compared to Bus 5 and Bus 67 for the four modes. Among the four modes, modes 1 and 3 are identified as inter-area oscillation modes, with their mode shape and participation factors shown in Fig. 8.

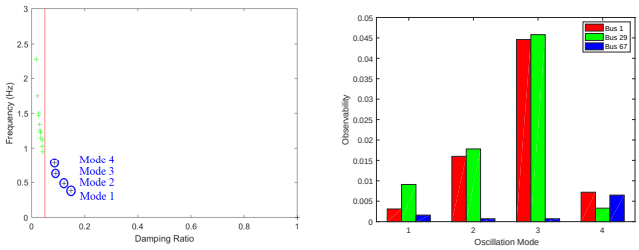

(a) (b)

Fig. 7: Observability of different buses. (a) Four low-frequency modes. (b) Buses 5, 29, and 67 observability of the four indicated modes.

The simulation data generated by PST is used for Prony analysis. The system order are set to be $n = 150$ and the sampling rate is defined to be 0.03 s. The singular values of the Hankel matrix D of buses 5, 29, and 67 are shown in Fig. 9. The singular value plots show that Bus 29 will result in best estimation accuracy. This finding corroborates with that from the observability shown in Fig. 7.

The reconstructed signals are presented in Fig. 10. It can be seen that the match of Bus 29 is better compared to that of Bus 5.

c) Sensitivity analysis of noise level: Bus 29's voltage measurement is polluted with uniformly distributed random noise. The singular value plots are generated (shown in Fig. 11) for the measurement with noise at signal noise ratio (SNR) of 80 dB, 40 dB, and 20 dB. Note that PMU data usually has

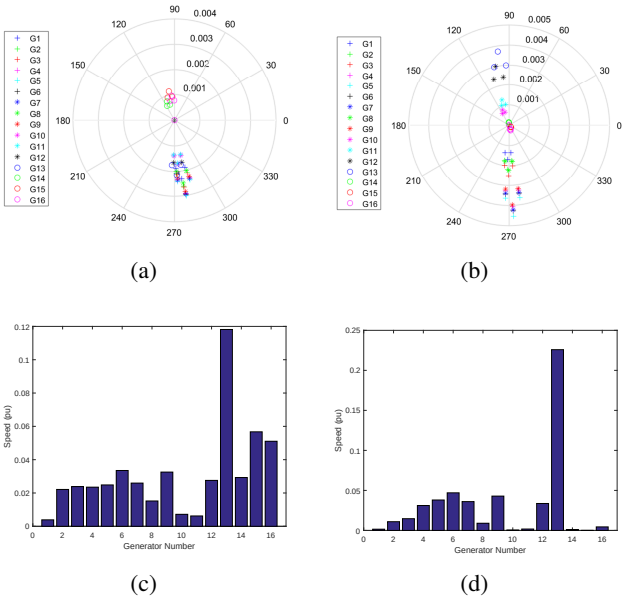

Fig. 8: Oscillation modes 1 and 3 participation factor of the 68-bus system. (a)Compass plot of rotor speed of mode 1 and (b)mode 3. (c)Real part of speed participation factor of mode 1 and (d)mode 3.

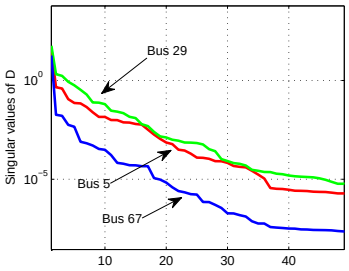

Fig. 9: Singular values of the Hankel matrix corresponding to bus voltage measurement at 5, 29, and 67.

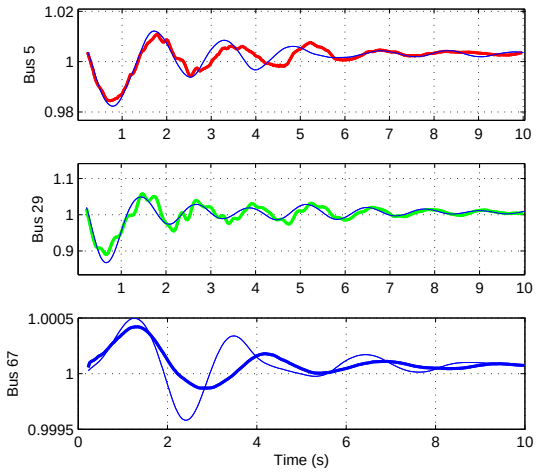

Fig. 10: Comparison of the reconstructed signals against the original measurements. Blue lines are the original measurements.

a SNR at 40 dB [14]. It can be clearly seen that large noise leads to inaccurate estimation.

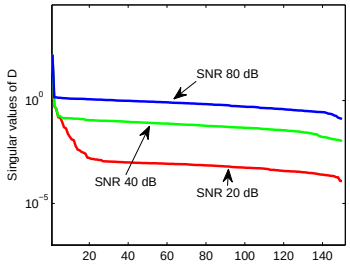

Fig. 11: Singular values of the Hankel matrix for different noise levels.

V. Conclusion

This paper demonstrates that the singular values of the Hankel matrix built for Prony analysis or ERA can serve as an indicator for estimation accuracy. Signals with large observability also show large singular values. In addition, influence of model order and noise level can also be demonstrated by the singular values. Two test cases, which are the two-area four-machine and the 16-machine 68-bus systems, are used to illustrated the relationship between singular values and dominant oscillation mode observability.

References

[1] M. Crow, M. Gibbard, A. Messina, J. Pierre, J. Sanchez-Gasca, D. Trudnowski, and D. Vowles, "Identification of electromechanical modes in power systems," *IEEE Task Force Report, Special Publication TP462*, 2012.

[2] J. Sanchez-Gasca and J. Chow, "Computation of power system low-order models from time domain simulations using a hankel matrix," *IEEE Transactions on Power Systems*, vol. 12, no. 4, pp. 1461–1467, 1997.

[3] J. F. Hauer, C. Demeure, and L. Scharf, "Initial results in prony analysis of power system response signals," *IEEE Transactions on power systems*, vol. 5, no. 1, pp. 80–89, 1990.

[4] D. Trudnowski, J. Johnson, and J. Hauer, "Making prony analysis more accurate using multiple signals," *Power Systems, IEEE Transactions on*, vol. 14, no. 1, pp. 226–231, 1999.

[5] L. Fan, "Data fusion-based distributed prony analysis," *Electric Power Systems Research*, vol. 143, pp. 634–642, 2017.

[6] N. Zhou, J. Pierre, and D. Trudnowski, "Some considerations in using prony analysis to estimate electromechanical modes," in *Power and Energy Society General Meeting (PES), 2013 IEEE*. IEEE, 2013, pp. 1–5.

[7] J.-H. Peng and N.-K. Nair, "Adaptive sampling scheme for monitoring oscillations using prony analysis," *IET generation, transmission & distribution*, vol. 3, no. 12, pp. 1052–1060, 2009.

[8] M. Dehghani, B. Shayanfard, and A. R. Khayatian, "Pmu ranking based on singular value decomposition of dynamic stability matrix," *IEEE Transactions on Power Systems*, vol. 28, no. 3, pp. 2263–2270, 2013.

[9] J. H. Chow and K. W. Cheung, "A toolbox for power system dynamics and control engineering education and research," *IEEE transactions on Power Systems*, vol. 7, no. 4, pp. 1559–1564, 1992.

[10] J. Khazaei, L. Fan, W. Jiang, and D. Manjure, "Distributed prony analysis for real-world pmu data," *Electric Power Systems Research*, vol. 133, pp. 113–120, 2016.

[11] J. H. Chow, A. Chakrabortty, L. Vanfretti, and M. Arcak, "Estimation of radial power system transfer path dynamic parameters using synchronized phasor data," *IEEE Transactions on Power Systems*, vol. 23, no. 2, pp. 564–571, 2008.

[12] P. W. Sauer, M. Pai, and J. H. Chow, *Power system dynamics and stability: with synchrophasor measurement and power system toolbox*. John Wiley & Sons, 2017.

[13] G. Rogers, *Power system oscillations*. Springer Science & Business Media, 2012.

[14] S. Brahma, R. Kavasseri, H. Cao, N. Chaudhuri, T. Alexopoulos, and Y. Cui, "Real-time identification of dynamic events in power systems using pmu data, and potential applicationsmodels, promises, and challenges," *IEEE Transactions on Power Delivery*, vol. 32, no. 1, pp. 294–301, 2017.